Cement & Concrete Composites 31 (2009) 647–657

Contents lists available at ScienceDirect

Cement & Concrete Composites

journal homepage: www.elsevier.com/locate/cemconcomp

Mechanical properties of hybrid fabrics in pultruded cement composites

Alva Peled [a,*], Barzin Mobasher [b], Zvi Cohen [c]

[a] Structural Engineering Department, Ben Gurion University, Beer Sheva, Israel
[b] Department of Civil and Environmental Engineering, Arizona State University, Tempe, AZ, USA
[c] Material Engineering Department, Ben Gurion University, Beer Sheva, Israel

ARTICLE INFO

Article history:
Received 6 November 2008
Received in revised form 23 April 2009
Accepted 16 June 2009
Available online 22 June 2009

Keywords:
Cement composites
Hybrid
Fabric
Tension
Textile
Pultrusion

ABSTRACT

This work concerns the tensile properties of cement-based hybrid composites manufactured as: (i) sandwich composites that combine different layers of single fabric types; and (ii) hybrid composites, made from several yarn types within the same fabric. Hybrid combinations of low-modulus fabrics of polyethylene (PE) or polypropylene (PP) and high-modulus AR glass or aramid fabrics were prepared by the pultrusion process and tested in tension. Influence of pultrusion direction on the results was one of the parameters studied. It was found that hybrid composites made from PE and AR glass sustain strains better than 100% AR glass composites, and are stronger than a single PE fabric composite. A hybrid fabric composites made with combination of high strength–high cost aramid and low stiffness–low cost PP yarns performed better than a single aramid fabric composite relative to their reinforcing volume contents. Results show that making hybrid composites is an attractive option for cement-based elements. The performance of hybrid fabric composites is also influenced by the arrangement of fabric layers in the laminates. Composites with brittle and relatively strong fabrics (glass) at the mid-section and ductile fabrics (PE) near the surfaces of the composite performed better in tension than composites with the opposite arrangement.

1. Introduction

There is a growing interest in the use of fabrics as reinforcement for thin sheet cement composites. In addition to ease of manufacturing, non-linear geometry of individual yarns within the fabric results in excellent bond development due to mechanical anchorage. These characteristics result in improved strength due to strain-hardening behavior even though the reinforcing yarns have a low modulus of elasticity [1,2]. A wide variety of fabric production methods such as weaving, knitting, braiding, and non-woven, make fabric design a flexible process. This flexibility enables controlling of fabric geometry, yarn geometry, and orientation of yarns in various directions as well as yarn material combinations (hybrid fabrics).

One way to produce fabric–cement elements is by a recently developed method, the pultrusion technique [3]. The pultrusion method allows design flexibility, fast construction time, enhanced mechanical properties, and aesthetic appeal of the final component. This technique enables production of thin sheet laminated composites for a wide range of applications, including wall panels, exterior siding, roofing tiles, flooring tiles, and pressure pipes.

Hybrid systems with two or more fiber materials are used to combine the benefits of each fiber into a single composite product. Strength and toughness optimization of hybrid thin sheet composites has been studied extensively using combination of different fiber types with low and high modulus of elasticity [4–11]. A high strength, high-modulus fiber primarily tends to increase the composite strength with nominal improvements in toughness. A low-modulus fiber can only be expected to improve toughness and ductility with limited improvement in composite strength. Combination of two or more types of fiber can produce a composite that is both strong and tough as compared to the mono-fabric type composite. Hybrid fiber reinforcement combinations can also be used in the manufacture of economically viable products by substituting economical fibers, such as polyethylene (PE) fibers, for more expensive alkali resistant (AR) glass fibers.

Xu et al. [4] reported that by using the concept of hybridization of glass, polypropylene, and polyvinyl alcohol (PVA) fibers, the resulting hybrid composite offered more attractive engineering properties than composites made with only one type of fiber. The hybrid system showed considerable improvements in ultimate tensile failure strain over the glass fiber composites. Similar conclusions were reported by Kobayashi and Cho [5] and Hasaba et al. [6] where steel and polyethylene hybrid combinations were studied. Kakemi et al. [7] evaluated the fracture of glass filaments in a hybrid polypropylene (PP)–glass composite. In the hybrid

* Corresponding author. Tel.: +972 8 6479672; fax: +972 8 6479670.
E-mail address: alvpeled@bgu.ac.il (A. Peled).

0958-9465/$ - see front matter © 2009 Elsevier Ltd. All rights reserved.
doi:10.1016/j.cemconcomp.2009.06.002

system, the fracture of the glass filaments was more evenly distributed than in the single glass composite, leading to greater strains at maximum stress of the hybrid composite. Mobasher et al. [8] found that the peak load of hybrid systems with carbon, aluminum and PP fibers increase as much as 75% over PP fiber composites or mortar. Perez-Pena and Mobasher [9] reported that the tensile ductility of cement composites containing polypropylene or glass mesh was significantly improved with various short fibers such as PP, AR glass, and nylon. Cyr et al. [10] reported that a hybrid composite with glass and PP fibers is stronger than a mono-PP fiber composite and tougher than a mono-glass fiber composite. Peled et al. [11] studied hybrid composites with combination of glass, PP and PVA microfibers. Combinations of 40:20:40 and 40:0:60 glass/PP/PVA (total of 5% vol. fiber reinforcement) were found to be similar in strength to 100% glass reinforcement but with a significant improvement in toughness.

In most cases discussed above, hybrid systems were studied with short fibers, randomly dispersed in the cement-based composite. In these cases there is a limitation in controlling the exact location of the fibers within the composite, which can be significantly important for many applications. The flexibility in fabric production enables several ways to combine two and more yarn materials within the fabric by controlling orientation and location of each material either in orthogonal or co-linear directions. One can utilize various yarn types at any direction within a fabric, or a combination of several fabric layers in a composite where each layer is made from different constituent materials. This approach provides full control of the exact location of each fabric and yarn, while their orientation in the composite during production allows for designing for specific characteristics as required by loading direction and magnitude. Therefore, the use of hybrid fiber reinforcement is particularly promising in fabric–cement composites.

In this study two types of hybrid composites were studied: (i) sandwich hybrid composites made with a combination of different layers of low-modulus fabrics of PE or PP and high-modulus AR glass fabric, and (ii) hybrid fabric composites combining PP and aramid yarns within a single fabric. All specimens were prepared by the pultrusion process [3,12]. The tensile behavior of the composites was studied using closed-loop uniaxial tension tests. The effect of various fabric types in suppressing the localization and crack bridging mechanisms as well as the microstructure were studied. Influence of the pultrusion direction on mechanical performance and microstructure was also evaluated.

2. Experimental program

2.1. Fabric types

2.1.1. Composite preparation

A pultrusion process [3,12], which allows production of laminated fabric–cement-based composites, was used. In this method the fabrics are passed through a slurry infiltration chamber, and then pulled through a set of rollers to squeeze the paste between the fabric openings while removing excessive paste. The fabric–cement composite laminate sheets are then formed on a plate shaped mandrel resulting in samples with width of 25 cm, length of 28 cm and thickness of about 1 cm. Two sets of specimens were prepared: (a) sandwich hybrid composites (made from fabrics of Set 1); and (b) composites with fabrics of Set 2, i.e., hybrid fabric (Tables 2 and 3).

Set 1. In the first system, two sets of cement board were prepared: (i) single (mono) fabric board made from eight layers of the single fabric type; and (ii) hybrid sandwich board where using four layers of AR glass fabric and four layers of either PE or PP-A. In order to study the effect of the pultrusion process, two types of mono-fabric composites were prepared: in the first the reinforcing yarns were along the pultrusion direction, and in the second the reinforcing yarns were perpendicular to the pultrusion process (Table 3).

Fig. 1 provides a schematic description of the sandwich hybrid composites, which were prepared as follows (Table 3):

(1) Two AR glass fabric layers were located at each surface of the composite (i.e., two layers at the bottom and two at the top) and four PE fabric layers were placed at the core of the board. These composites are referred to as G–PE–G.
(2) Same as the previous composite, except that PP-A fabrics were located at the core of the composite (G–PP–G).
(3) Two PE fabric layers were located at each surface of the composite and four AR glass fabric layers were placed at the middle of the board (PE–G–PE).
(4) Same as the previous composite, except that two PP-A fabric layers were located at each surface of the composite (PP–G–PP).

Table 1
Properties and geometry of yarns made up the fabrics.

Yarn type	Yarn nature	Tensile strength (MPa)	Modulus of elasticity (MPa)	Filament size (mm)	Bundle diameter (mm)	Number of filaments per bundle
AR glass	Bundle (coated)	1360	78,000	0.014	0.80	–
PE	Monofilament	260	1760	0.250	0.25	1
PP-A	Bundle	500	6900	0.016	0.12	158
PP-B	Bundle	220	7000	0.039	0.70	315
Aramid	Bundle	2370	55,000	0.012	0.38	1106

Table 2
Fabric composition and geometry.

Set #	Yarn type	Fabric structure	Yarn density per cm	
			Reinforcing yarns	Perpendicular yarns
1	AR glass	Bonded	4.0	4.0
	PE	Woven	22	6
	PP-A	Warp knitted	8.0	0.8
2	PP-B	Warp knitted	2.5	2.5
	Aramid	Warp knitted	2.5	2.5
	Hybrid: PP-B and aramid	Warp knitted	2.5	2.5

Table 3
Specimen types.

Set #	Fabric type	Yarn type	Number of layers	Layer locations	Direction of testing vs. pultrusion direction
1	Mono	PP-A	8	Throughout thickness	Parallel (0°)
1	Mono	AR glass	8	Throughout thickness	Parallel (0°)
1	Mono	PP-A	8	Throughout thickness	Perpendicular (90°)
1	Mono	AR glass	8	Throughout thickness	Perpendicular (90°)
2	Mono	Aramid	3	Throughout thickness	Parallel (0°)
2	Mono	PP-B	3	Throughout thickness	Parallel (0°)
1	Hybrid	PP-A Glass	4 4	Surfaces Core	Parallel (0°)
1	Hybrid	Glass PP-A	4 4	Surfaces Core	Parallel (0°)
1	Hybrid	PE Glass	4 4	Surfaces Core	Parallel (0°)
1	Hybrid	Glass PE	4 4	Surfaces Core	Parallel (0°)
2	Hybrid	PP-B + aramid	3	Throughout thickness	Parallel (0°)

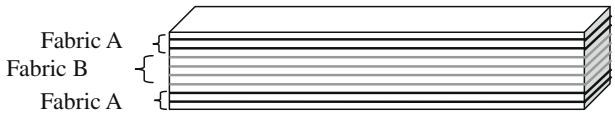

Fig. 1. Schematic description of the hybrid laminated composite.

In all these cases the matrix was made from 6473 gr (42% by vol.) cement, 560 gr (5% by vol.) silica fume and 10 ml (0.1% by vol.) superplasticizer, with $w/c = 0.37$, by wt. The specimens were demolded at 24 h after casting and at least five specimens from each system were prepared for testing. The specimens were cured for 3 days at 80 °C, 100% RH and then stored in room environment until testing in tension at 7 days after the pultrusion process.

Set 2. In the second system, each cement board was made of three layers of identical fabric types, either PP-B or aramid (Table 3). Hybrid composite boards were prepared using the hybrid fabric, containing PP-B and aramid yarns (within the same fabric, Table 2) for all three layers. Cement paste with $w/c = 0.4$ by weight was used to produce this set of specimens. The samples were cured at 100% relative humidity (RH) at room temperature for 25 days. At the end of the curing period, the specimens were kept at room temperature for another 3 days until tested in tension. Preliminary testing indicated that the tensile results of accelerated curing (as in Set 1) and normal curing (as in Set 2) were quite similar, therefore the two sets of specimens can be discussed together.

3. Testing

3.1. Tensile tests

Tensile stress–strain behavior of the composites was studied using uniaxial tension tests conducted on a closed-loop control MTS testing machine with a capacity of 89 kN. The rate of cross head displacement was set at 0.008 mm/s. Metal plates with dimension of 25 × 50 mm and 1 mm thick were glued on the gripping edges of the specimen to minimize localized damage and allow better load transfer from the grips. The samples were held using hydraulic grips operated at low pressure to avoid localized crushing, hence in consideration to the stroke control mode of loading, the boundary condition of the testing was best characterized by an imposed displacement of a fixed boundary. The free length between the grips of the specimen was 180 mm. At least five replicate samples of each category were tested and results reflect the average and standard deviation values. Typical stress–strain curves representing the tensile behavior of individual composites were chosen for comparison.

Several properties of the composite were determined: (1) initial modulus (within the elastic region); (2) post-cracking tensile strength; and (3) toughness (measured as the area under the stress strain curve, up to a strain of 7% when applicable).

3.2. Crack spacing measurements

Throughout the tensile testing, parallel distributed cracks formed along the length of the specimen. The continuous formation of these cracks was recorded at 15 s intervals using a high resolution camera and a digital frame grabber. Using digital processing toolbox of MATLAB® the images were processed to quantitatively measure the crack spacing and density as a function of the applied strain. The average crack spacing for each strain level was correlated with the stress–strain response. The stress–strain response was also used to calculate the tangent stiffness at several designated strain levels for the PE, glass and PP-A single fabric composites. Results of stiffness degradation were correlated with the crack spacing data. Details regarding the procedures described can be found in an earlier publication [13].

3.3. Crack pattern observations

The cracking pattern was also studied by optical fluorescent microscopy. Matrix, interface and distributed cracking modes were observed for the single and hybrid systems along the length, thickness, and internal sections of the laminated composites.

3.4. Microstructure characteristics

Microstructure characteristics of the different composites were observed using a JOEL-840 Scanning Electron Microscope (SEM). For these observations, fragments of specimens obtained after tensile tests were dried at 60 °C and gold-coated. Microstructural features such as matrix penetration between the opening of the fabrics and between the bundle filaments were evaluated.

4. Results

4.1. Mono-fabric composites (Set 1)

4.1.1. Effect of fabric type

Summary of average tensile results of the different composites made from Set 1 fabrics (Table 2) are shown in Table 4. Fig. 2a

Table 4
Tensile properties of the different composites of the laminated hybrids (Set 1).

Specimen type	Young modulus (MPa)	Tensile strength (MPa)	Ultimate strain (mm/mm)	Toughness (MPa)
PE	4040	7.0 (0.5)[b]	0.075	0.408
Glass (0°)	3668	20.05 (2.74)[b]	0.030	0.359
PP-A (0°)	4631	24.0 (0.50)[b]	0.075	1.424
[a]Glass 90°	5818	12.0 (1.0)[b]	0.013	0.128
[a]PP-A 90°	3221	13.4 (5.4)[b]	0.070	0.668
PE–G–PE	2822	12.6 (1.8)[b]	0.027	0.327
G–PE–G	3183	9.3 (0.6)[b]	0.024	0.397
PP–G–PP	6136	14.6 (1.9)[b]	0.053	0.695
G–PP–G	5904	14.4 (1.9)[b]	0.050	0.609

[a] The reinforcing yarns are perpendicular to the pultrusion direction.
[b] Numbers in brackets are the standard deviation.

shows the stiffness degradation during tensile testing as a function of crack spacing for PE, AR glass, and PP-A mono-fabric systems. A general decreasing trend of tangent stiffness and crack spacing as a function of applied strain is observed for all cases. The reduction in stiffness at low strains (high crack spacing) is significant for all fabrics, especially polymeric systems. The AR glass composite shows the highest stiffness retention values. The lowest stiffness values are reported for the PE fabric composite. Trends of stiffness degradation of the PP-A composites show higher stiffness values than the PE system during the entire loading. Such trends are expected and correlate well with the modulus of elasticity of the different fabric systems (Table 1). Differences in stiffness values were used as the basis of fabric selection for preparation of laminated composites and will be discussed in the following sections. The main goal was to combine low and high stiffness systems in order to observe potential synergistic effects.

Fig. 2b compares the behavior of AR glass composites with the PE composite system. The high-strength glass composite shows a relatively brittle behavior, as compared to the more ductile behavior of the PE composite. These results are expected due to the differences in stiffness and ductility of glass and PE (Table 1). It should be noted that while the PP-A fabric has a lower modulus of elasticity and strength than that of glass, its tensile behavior at strains above 5%, is much greater than that of the glass and PE fabric composites (Table 1). The improved performance is observed in both strength and toughness and may be explained based on the microstructure of the different composites. As presented in Fig. 3, the SEM micrographs of the composites with the PE, AR glass, and PP-A fabrics show the different geometry of fabrics used.

The PE has the highest density among the other two fabrics; however due to monofilament nature of its yarns, a relatively small surface contact area with the cement paste matrix is obtained (Fig. 3a). In this woven fabric, the two sets of warp and fill yarns are allowed to slide by friction while they pass under and above each other. The crimp shape of the yarns in this fabric results in strong mechanical anchoring with the cement matrix but the monofilament nature of the yarns has a reduced bond as compared with the multifilament PP-A fabric. This parameter may explain the low performance of the yarns made with PE fabric (Table 1).

The glass fabric is relatively open and its yarns are bonded at the junction points providing strong connections between its two sets of yarns (Fig. 3b). The sizing on the glass yarns prevents cement matrix penetration between the filaments of the bundle. The stiff and strong junctions of the glass fabric contribute to the mechanical performance of the composite [14]; however, the coating of the bundles may be detrimental from a bonding point of view, since only the perimeter of the bundle is in contact with the cement matrix.

In the knitted PP-A fabric the reinforcing yarns have a multifilament nature (Fig. 3c), and are connected by stitches (loops) at the junction points. The cement matrix penetrates between the filaments of the bundle providing large surface area and improved bonding. However, such improved bonding can take place only if the bundles within the fabric are sufficiently open to allow matrix penetration; the stitches in the knit fabric may tightly hold the bundles and reduce paste penetrability. Such low penetrability is

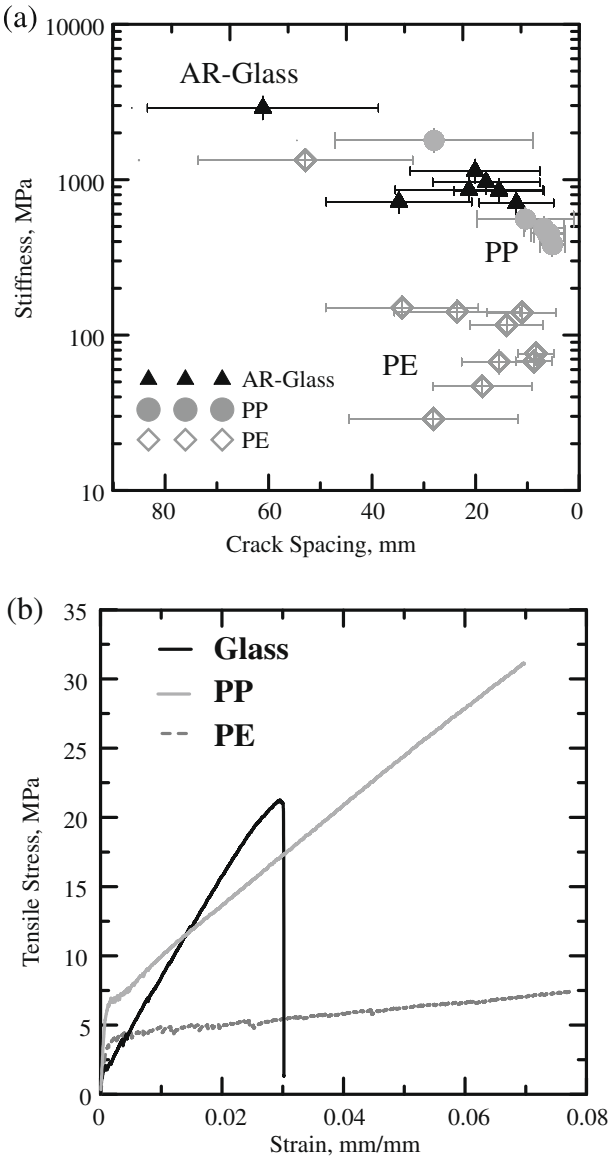

Fig. 2. Tensile properties of the composites with the different fabrics: (a) composite stiffness vs. crack spacing and (b) stress–strain response.

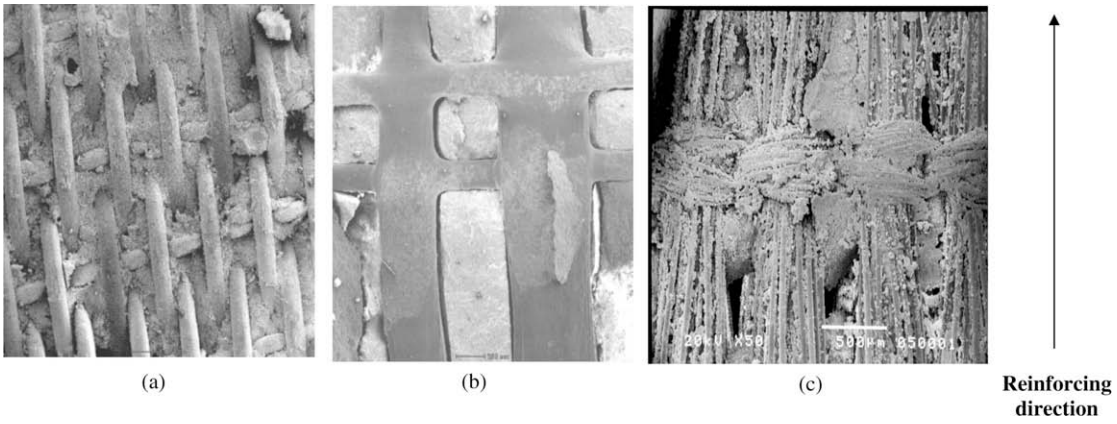

Fig. 3. SEM observations of the composites with the different fabrics: (a) PE, (b) AR glass, and (c) PP-A.

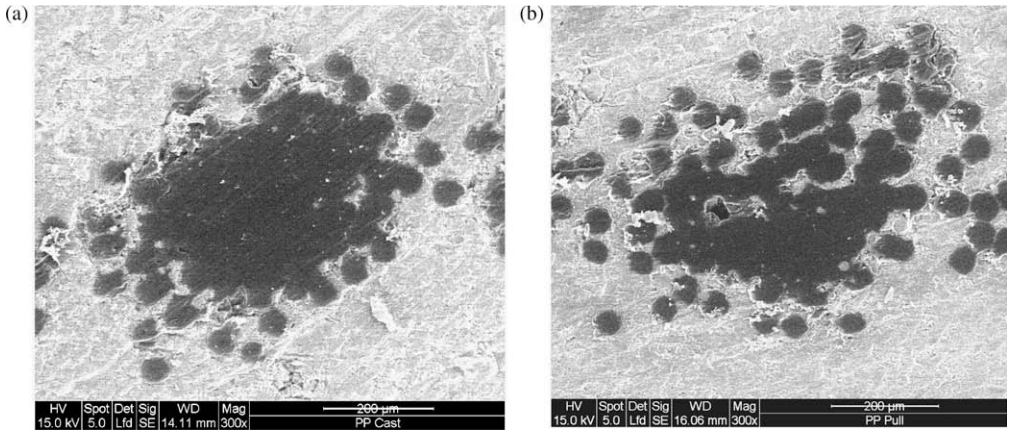

Fig. 4. Cross sections of PP-A fabrics in cement matrix produced by different methods: (a) hand lay up of fabric and (b) impregnated fabric (pultrusion).

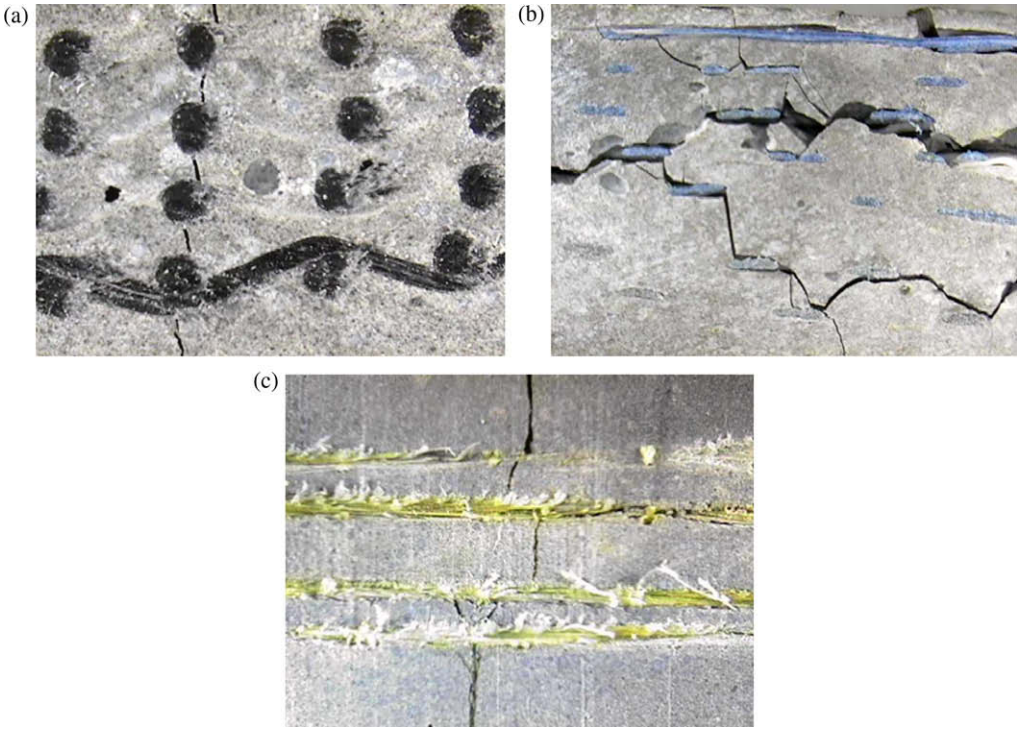

Fig. 5. Crack pattern of the different composites (side view): (a) glass (b) PE, and (c) PP-A.

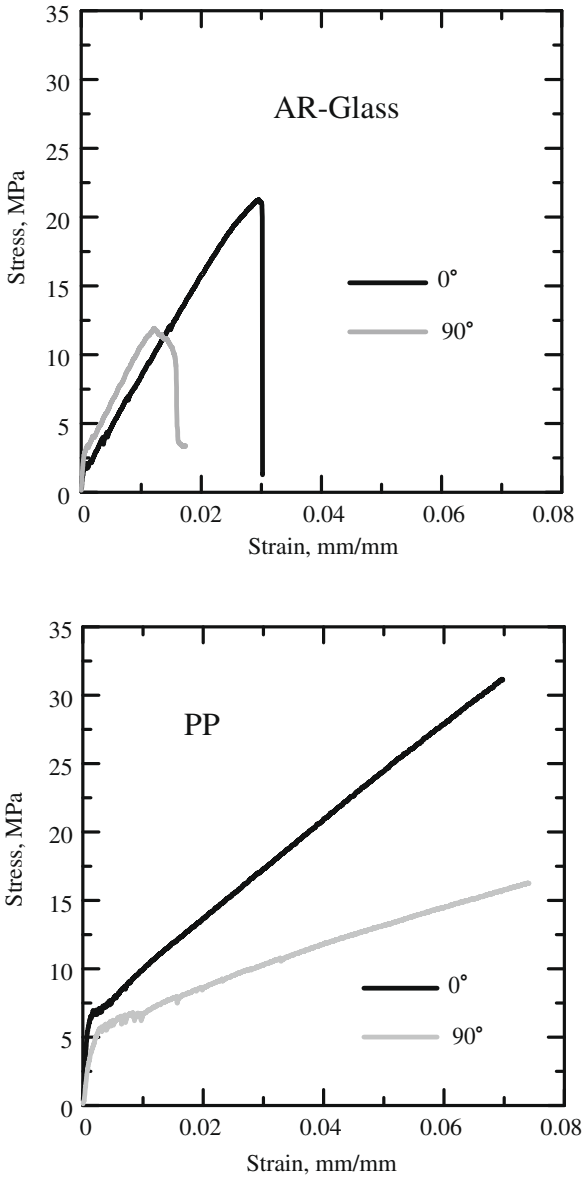

Fig. 6. Tensile behavior of composites where the reinforcing yarns of the fabrics are located along the pultrusion direction and transverse to the pultrusion direction for (a) glass and (b) PP-A fabrics.

clearly observed in Fig. 4a which shows the cross-section of a bundle within PP-A knit fabric prepared using a manual fabrication process. The pultrusion process enables high shear penetration of the cement paste between the opening of the bundle filaments as observed in Fig. 4b. Such improved penetration provides strong bonding with the cement matrix, leading to the improved performance of the PP-A fabric composite (Fig. 2b).

The diversity in behavior of the various fabric composites is also observed by comparing the crack patterns during tensile loading, as presented in Fig. 5. The cracking of the PE composites is developed along the weak planes, i.e., at the high curvature junction points of the reinforcing crimped yarns (Fig. 5a). During tensile tests the crimped reinforcing yarns are stretched and aligned causing stress concentrations at the matrix near the vicinity of the high curvature points; the perpendicular yarns at these areas can cause further weakening of the matrix, thus explaining the behavior of some of the low performance PE composites (Fig. 2b). A relatively large extent of cracking throughout the specimen is observed with the glass composite as shown in Fig. 5b (which is a side view along the reinforcing yarns). The cracks develop at the weak points of the composite, where the perpendicular yarns are located. No such large cracking is observed with the PP-A composite (Fig. 5c) and the crack arrest mechanism of the reinforcing yarns is clear in this figure, which correlate well with the improved mechanical behavior (Fig. 2b).

4.1.2. Effects of processing direction

Fig. 6 compares the tensile behavior of composites with monofabrics, PP-A and AR glass, where the reinforcing yarns are placed parallel and perpendicular to the pultrusion direction. In both cases the tensile test was performed along the direction of reinforcing yarns, i.e., along the straight yarns and perpendicular to the stitches (Fig. 3c). The difference in behavior of the two composites is obvious and shows that while the same yarns are strained during testing, the composite is stronger in the pultrusion direction and relatively weak in the direction transverse to the pultrusion process. This behavior is observed for both glass and PP-A fabrics, indicating that the mechanical behavior of the composite improves in the pultrusion machine direction.

Comparison of the microstructure of these composites explains the differences in behavior (Fig. 7). In the case of the glass fabric it is observed that the surface of the reinforcing yarn perpendicular to the pultrusion direction is smooth and fully coated with the sizing (Fig. 7b). On the other hand, when the reinforcing yarn is along the pultrusion direction its surface is relatively rough and the filaments are partly exposed out of the coating (Fig. 7a). This roughness of the reinforcing yarns may occur due to the intensive frictional shear forces which are applied to the yarns during the impregnation process. Such rough surfaces may provide mechanical anchorage of the yarns with improved bonding and mechanical performance (Fig. 6a – curve 0). However, when the reinforcing yarns are transverse to the pultrusion direction they are not subjected to such intensive forces and therefore their surface remain smooth (Fig. 7b), resulting in lower mechanical anchorage (Fig. 6a – curve 90). In the case of the PP-A fabric the reinforcing yarns are in a multifilament form, when these yarns are passed along the impregnation process, the matrix can penetrate in between the filaments (Fig. 7c), causing better bonding due to mechanical anchorage and greater tensile performance (Fig. 6b). However, when these yarns pass through the impregnation bath along the 90° direction, they cannot fill completely with the cement matrix (Fig. 7d) leading to poor bonding and reduced tensile properties (Fig. 6b).

4.2. Hybrid composites

4.2.1. Sandwich composites (Set 1)

Combining the brittle and strong glass system with the ductile PE fabrics (fabrics in Set 1, Tables 2 and 3) can lead to a composite stronger than the PE and more ductile than the glass fabric systems. The improved strength of such combination is evident in Fig. 8, which shows the tensile behavior of the hybrid composites with PE and glass fabrics as compared with the PE system alone. The strength of the hybrid systems is greater than that of the PE system for both hybrid composites, regardless of the location of glass layers: at the two surfaces or at the core of the laminated composite. The increase in strength is as much as twice that of a mono-PE system. The strength of both hybrid systems are however lower than that of the AR glass (Table 4). The ductile behavior of the hybrid composites (Fig. 8) can compare with the glass composite shown in Fig. 2b. The strain capacity increases from about 0.03 mm/mm for the glass composites to above 0.08 mm/mm for the G–PE–G hybrid composite (Fig. 8b). The increase in strain capacity observed for the PE–G–PE hybrid composite (Fig. 8a) is not as significant though.

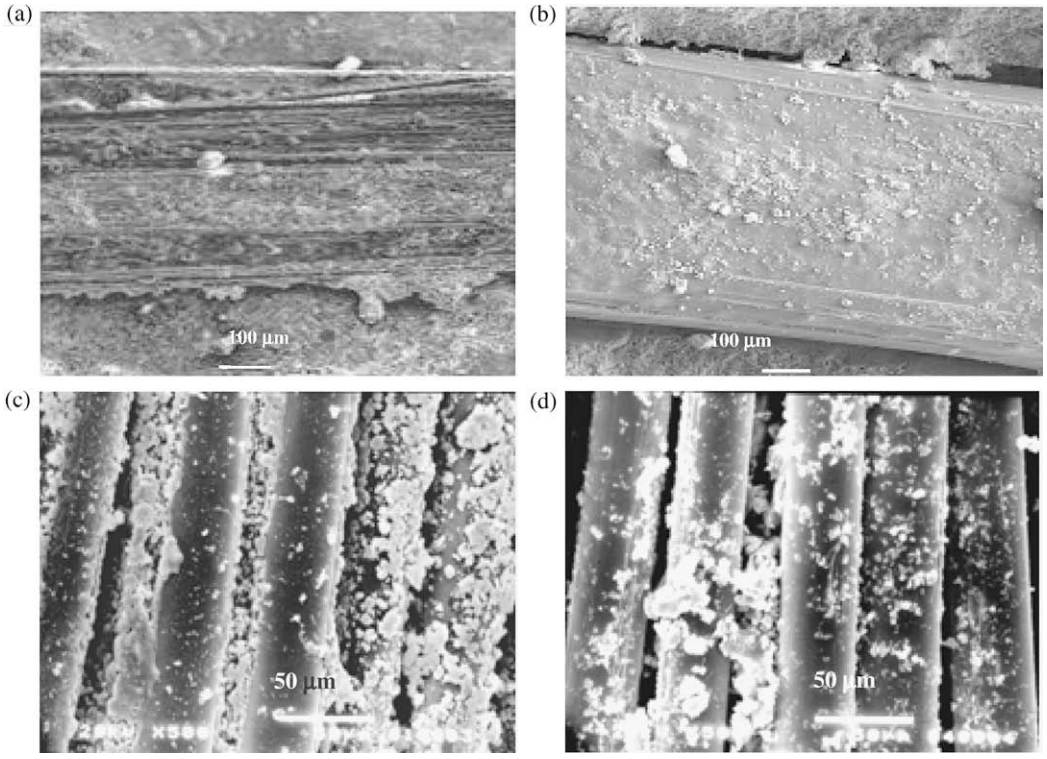

Fig. 7. Reinforcing yarns of the fabric in the cement matrix after specimen production by the pultrusion process: (a) glass along the pultrusion, (b) glass perpendicular to the pultrusion, (c) PP-A along the pultrusion, and (d) PP-A perpendicular to the pultrusion direction.

The tensile behavior of hybrid systems is influenced by the material combinations in addition to their arrangement across the thickness, i.e., whether the ductile material is placed at the surfaces or at the center of the sandwich composite (Fig. 1). The differences in behavior of two hybrid composites made from four layers of glass fabric and four layers of PE fabric, but with different lay up structures, are presented in Fig. 9. When the ductile fabrics are at the surface of the composite and the strong brittle fabrics are located at the middle (PE–G–PE), the tensile behavior is improved in comparison to composites with the opposite arrangement (G–PE–G). The improvements in strength and toughness are about 40% and 20%, respectively (Table 4). This behavior can be attributed to better transfer of the load from the weak exterior layers to the strong interior layers, resulting in improved crack arrest mechanisms by the interior layers of the stronger fabric. These effects will be discussed in detail later.

The crack spacing developed during loading is shown in Fig. 8 as a function of applied strain. Results of both the sandwich hybrid systems and the single PE system are presented. At low strain levels (<0.02), the crack spacing is smaller for the PE–G–PE hybrid as compared with the PE composite; at higher strain levels, however, major differences in crack spacing between the two systems are not observed (Fig. 8a). Comparison of all single fabric and hybrid systems shows relatively large spacing between the cracks of the G–PE–G composite along the entire loading as compared to other composites (Fig. 10), indicating a less efficient reinforcing system. The larger crack spacing in the G–PE–G system than that of single fabric composites of PE and glass suggests that the efficiency of load transfer in hybrid sandwich system with glass at the two surfaces of the composite and PE at the core is less effective than composites made of single fabric or hybrid where the PE is at the surfaces and glass at the core. In general, the G–PE–G composites have a higher bending stiffness than PE–G–PE composites, suggesting that small misalignment in the tensile testing leads to cracking of the strong and stiff layers, whereas in the PE–G–PE composites, the weaker, more ductile layers are protecting the internal glass lamina and reducing bending during the tension test. The stress transfer from matrix to fabrics in G–PE–G system is limited and may explain the lower tensile behavior as well as the larger crack spacing of these systems as compared with the PE–G–PE composite (Fig. 9).

During the loading stages where no new cracks are formed, the crack widening process can be observed as shown in Fig. 10. The crack widening for the PE fabric composite and the PE–G–PE hybrid system begins at a strain level of less than 2%, whereas for the G–PE–G hybrid it is observed at a larger strain of around 3%.

The pattern of the developed cracks in the glass–PE hybrid composites is presented in Fig. 11. It is observed that the crack pattern at the glass fabric is different than at the PE fabrics. In the case of PE–G–PE composite (Fig. 11a) wide cracks are observed at the glass zone (middle of the composite) whereas smaller cracks are observed at the PE zones at the top and bottom of the composite. Delamination between the glass zone and the PE zone is clearly observed (at the top of Fig. 11a). Such delaminations occur due to the differences in the stiffness of the PE and glass fabrics, as the PE can sustain much larger strains than the glass. During tensile loading, the PE is highly strained while the change in the length of the glass fabric is much smaller, leading to separation and sliding between the two fabric regions. Larger separation between the glass and PE zones is observed with the G–PE–G hybrid composite (Fig. 11b), where the ductile PE fabric is located at the center and the glass is at the surfaces of the composite. When the four layers of the strong glass fabrics are located together at the center of the composite and tensioned, they are less susceptible to bending leading to greater tensile response. However, when these four layers of the glass fabrics are separated and located at the faces of the composite, the performances are reduced (Fig. 9). This observation can be further explained by the geometrical considerations that when

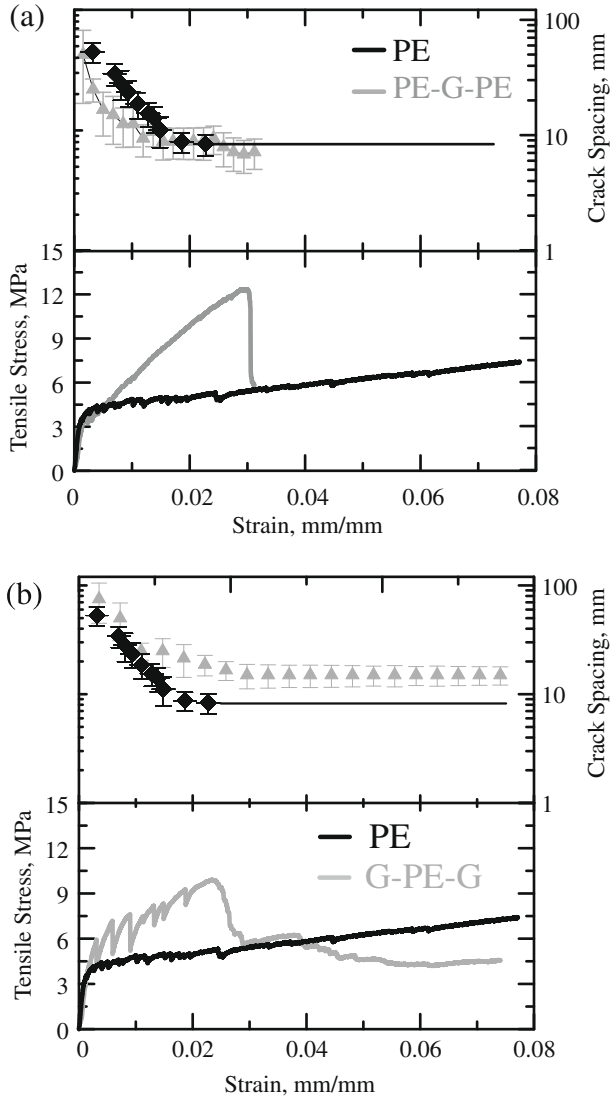

Fig. 8. Tensile behavior and crack spacing of hybrid sandwich PE and glass composites compared with mono-PE composite: (a) PE–G–PE hybrid and (b) G–PE–G hybrid.

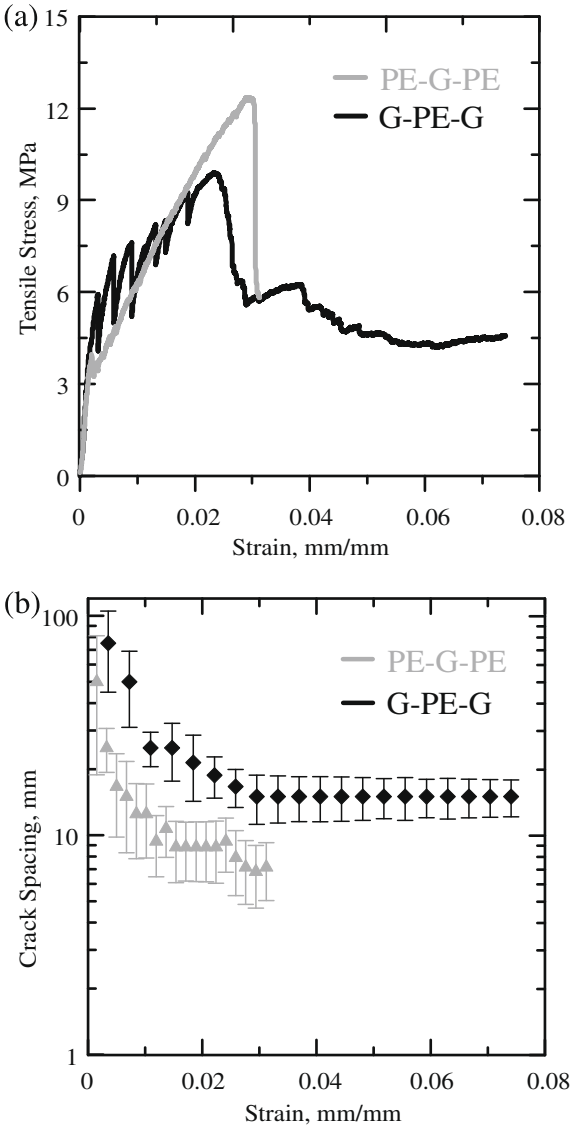

Fig. 9. Tensile behavior of the PE–glass hybrid sandwich composites: (a) stress–strain response and (b) crack spacing behavior during loading.

the strong layers are placed at the surfaces, the specimen becomes much stiffer from a flexural standpoint. While the axial stiffness remains unchanged from the first principles point of view, the ratio of axial to flexural stiffness of the sample decreases. This indicates that the test results are affected by several factors. When tests are conducted under a displacement controlled mode in tension, the slightest misalignment of the sample, or imperfection such as thickness differences between the layers, may result in generation of spurious flexural loads causing bending and premature failure of the specimen. For tension applications, PE–G–PE composites are much more suitable, where as in bending G–PE–G composites are preferable. By applying the assumptions of plane sections remaining plane as applicable to these composite systems in bending, one can deduce that stiffer layers at the extreme fibers will contribute to higher flexural stiffness and strength as shown in earlier work [13,15]. This observation can also be evaluated in the context of axial load–displacement diagrams of the two sets of samples compared. Note that there is more uniformity in response of PE–G–PE samples than that of the G–PE–G samples. PE–G–PE samples are less sensitive to the imperfections under axial load conditions as compared to the G–PE–G specimens. The high strain

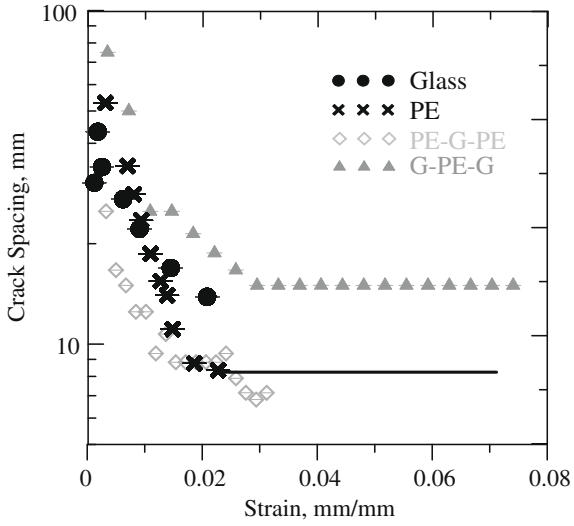

Fig. 10. Crack spacing vs. strain of the hybrid PE–glass composites compared with the mono-fabric composites, glass, and PE.

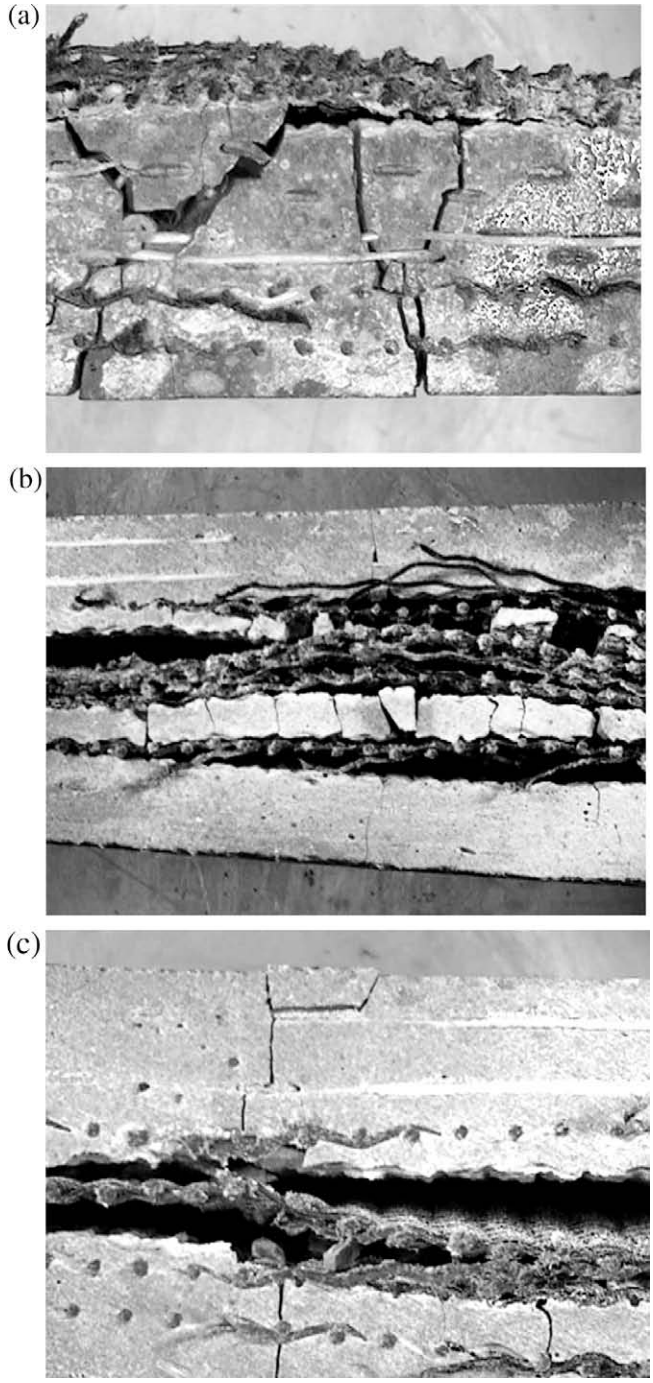

Fig. 11. Crack pattern of glass–PE hybrid composites, side view on longitudinal section: (a) PE–G–PE and (b and c) G–PE–G.

capacity of the PE fabric systems allows for their deformation and transfer of the load back into the glass samples. The placement of PE fabrics in the middle of the layer, while more beneficial in the flexural mode of loading, is not as effective under tensile conditions.

The tensile behavior of hybrid composites containing glass and PP-A fabrics is presented in Fig. 12. As shown in Fig. 12a, mono-glass and PP fabric composites are compared with PP–G–PP hybrid composite. The PP–G–PP hybrid composite is more ductile than the glass composite but does not show any significant advantage when compared with the mono-fabric PP composites. No significant difference in tensile behavior is observed between PP-A glass hybrids

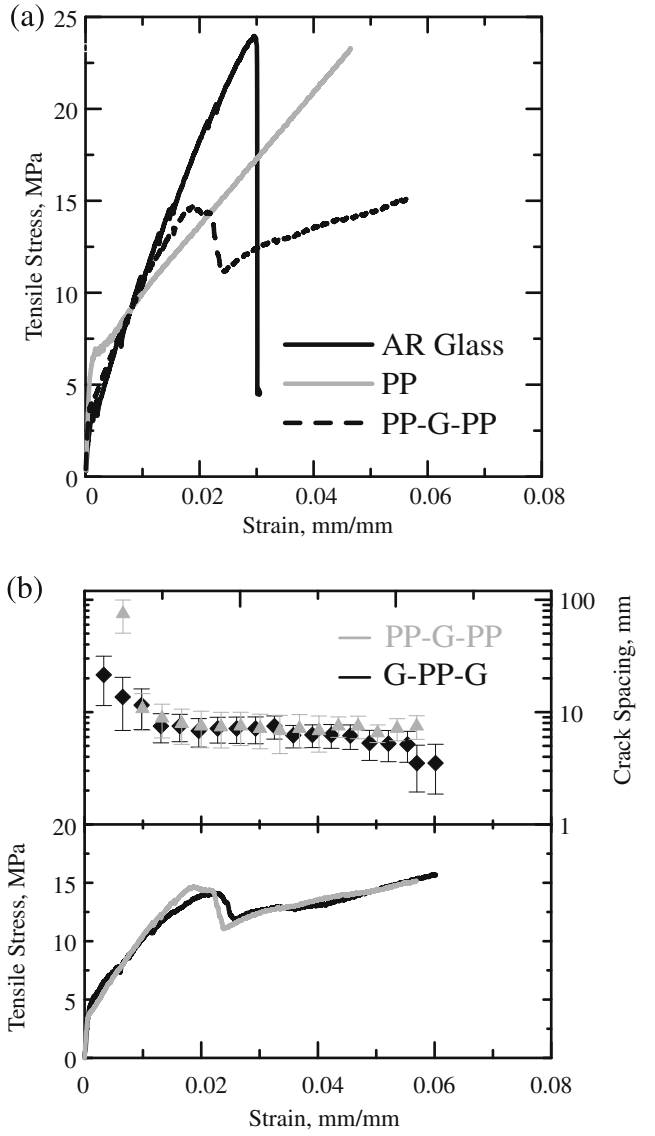

Fig. 12. Tensile behavior of glass–PP hybrid composites: (a) hybrid PP–G–PP compared with mono-PP and glass composites and (b) comparison of hybrid with different arrangement of the fabrics.

(PP–G–PP and G–PP–G), as seen in Fig. 12b. The crack spacing is also nearly the same for both hybrid composites throughout the entire loading, and no significant difference in the crack pattern is seen between the two (Fig. 13). No delamination is observed between the glass and PP laminates in both hybrid systems, suggesting good contact between the glass and the PP zones.

It should be noted that although the properties of the PE and PP-A yarns are relatively similar, the geometry of these two yarns are completely different; the PE yarn is a relatively thick monofilament whereas the PP-A is a bundle containing many filaments (Table 1). These differences in geometry can influence the bond developed with the cement matrix: poor bond with a single PE yarn and stronger bond with the tiny filaments of the PP-A bundle. This is even more pronounced when the pultrusion process is used [3,12]. Thus, the reinforcement efficiency of the PP-A fabric is higher than PE fabric. It was also demonstrated that the composite performance of the PP-A fabric is quite similar to that of the AR glass fabric composite (Fig. 12a). This similarity in overall stiffness helps in limiting the delamination potential between the two fabric layers as observed in Fig. 13, since the difference in behavior between

Fig. 13. Crack pattern of hybrid composite PP–G–PP, side view on longitudinal section.

the two fabric segments is greater with the PE-G systems than for the PP-G composites. These differences in behavior may explain, at least to some extent, the difference in lamina lay up that cause significant changes in G–PE hybrids while only marginal changes in PP–G hybrid systems.

4.2.2. Hybrid fabric composite (Set 2)

In this case the composites were produced with the fabrics in Set 2, aramid and PP-B (Table 2). The hybrid fabric concepts in this study combined ductile, low cost yarns with the more expensive, stiff yarns. The tensile behavior of the composite reinforced with the hybrid fabric is presented in Fig. 14, along with the tensile response of mono-PP and mono-aramid fabric composites. The properties of these composites are presented in Table 5. The hybrid composites performed similar to mono-aramid fabric composite in terms of strength, although 50% of the aramid yarns were replaced with PP. Moreover, hybrid composites exhibited much better tensile behavior than PP composites. The toughness of the

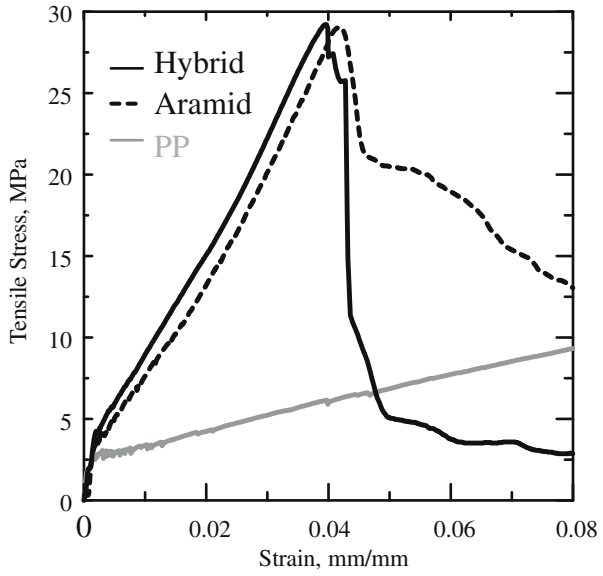

Fig. 14. Tensile behavior of composites reinforced with aramid fabrics, PP-B fabrics and hybrid fabric containing PP and aramid yarns.

Table 5
Tensile properties of the different composites of the aramid + PP-B hybrid (Set 2).

	Volume fraction V_f (%)	Tensile strength (MPa)	Efficiency factor of strength	Ultimate strain (mm/mm)	Toughness (MPa)
Aramid	1.9	26.2 (8.83)[a]	0.58	0.037	0.717
PP-B	6.2	9.25 (0.72)[a]	0.67	0.070	0.466
Hybrid	2.6	25.75 (4.98)[a]	0.94	0.063	0.677

[a] Numbers in brackets are the standard deviation.

hybrid composite is also similar to that of the mono-aramid composites and much greater than that of the mono-PP-B composite. The improved toughness of the hybrid system over that of the mono-PP-B composite is about 30% and the improved strength is almost 300%. It is noted that the total volume content of the reinforcement yarns in the hybrid fabric composite was 2.6%, which was slightly above that of the mono-aramid fabric composite (1.9%) but significantly lower than that of the mono-PP-B fabric composite (6.2%). In addition, in the hybrid composite, the aramid content was only 1.0% and that of the PP-B was 1.6%. Since the aramid yarns are about thirty times more expensive than PP yarns, hybridization is a cost effective system with energy properties similar to those of the mono-aramid composite.

The superiority of the hybrid composite was obvious when comparing its efficiency factor with those of the mono-aramid and PP-B composites (Table 5). The efficiency factor was calculated as the ratio between the tensile strength of the composite and the tensile strength of the yarn making up the fabric (Table 1) weighted by its volume fraction ($\sigma_{composite}/(\sigma_{yarn}*V_f)$). This was done to compare the different systems on a similar basis, and to verify the beneficial effects of hybridization. An improvement of as much as 90% was observed for the hybrid composite when compared with the efficiency factor of the mono-aramid composites. The hybrid also exhibits greater efficiency factor than that of the mono-PP-B composite. No delamination was observed with the hybrid fabric system and the composite behaved as a homogenous unit. These observations and trends clearly point out the advantage of hybrid fabrics as reinforcement for cement composite applications.

5. Summary and conclusions

Hybrid composites can be manufactured by different methods. Different fabric types can be combined as individual layers in the construction of a lamina. Alternatively, different yarns can be combined in the construction of a single hybrid fabric. In this study both hybrid systems showed advantages as reinforcement for cement-based composites:

- The sandwich hybrid systems made from brittle glass fabrics and ductile PE fabrics performed better than glass composites in their ability to sustain strains and was stronger than mono-PE fabric composites.
- The tensile performance of hybrid fabric composites are influenced not only by material combination but also by the arrangement of the fabric layers in the composite laminates. A hybrid composite with arrangement of brittle and strong fabrics at the center of the composite and ductile fabrics at the surfaces of the composite performed better in tension than a composite with the opposite arrangement, i.e., ductile fabrics at the center and strong/stiff fabrics at the surfaces.
- Combining aramid and PP yarns in a hybrid fabric with equal proportions exhibited similar behavior to those of the mono-aramid composite. Although its volume content of reinforce-

ment was much lower, the hybrid composite performed much better than the mono-PP fabric composite, with a similar volume fraction V_f of 6.2%. In this manner the different yarn types are connected to the same fabric unit, which can limit delamination.

PP fabric composites showed an optimum load carrying capacity at large strain levels as high as 5%. Glass fabric composites maintained a high stiffness over strain ranges of up to 2%. Combinations of PP and glass fabrics gave composites with better ductility than a mono-glass composite, but did not show any benefit in performance compared with the mono-PP composite.

The direction of the pultrusion process had a significant influence on the mechanical performance indicating that this process makes orthotropic samples with properties that are much better along the pultrusion direction than perpendicular to it, even when the same reinforcing yarns are located in each direction.

Acknowledgements

The authors thank Nippon Electric Glass Co., Ltd., and Institute of Textile Technology at RWTH, Aachen (ITA) for their cooperation and for providing the fabrics used in this study. The BSF (United States Israel Binational Science Foundation) Program 2006098 is acknowledged for the financial support of this research.

References

[1] Peled A, Bentur A, Yankelevsky D. Effect of woven fabrics geometry on the bonding performance of cementitious composites: mechanical performance. Adv Cem Based Mater J 1998;7(1):20–7.
[2] Peled A, Bentur A. Fabric structure and its reinforcing efficiency in textile reinforced cement composites. Compos A J 2003;34:107–18.
[3] Peled A, Mobasher B. Pultruded fabric–cement composites. ACI Mater J 2005;102(1):15–23.
[4] Xu G, Magnani S, Hannant DJ. Tensile behavior of fiber–cement hybrid composites containing polyvinyl alcohol fiber yarns. ACI Mater J 1998;95(6):667–74.
[5] Kobayashi K, Cho R. Flexural characteristics of steel fibre and polyethylene fibre hybrid – reinforced concrete. Composites 1982;13:164–8.
[6] Hasaba S, Kawamura M, Koizumi T, Takemoto K. Resistibility against impact load and deformation characteristics under bending load in polymer and hybrid (polymer and steel) fiber reinforced concrete. In: Hoff GC, editor. ACI SP-81. Detroit: Fiber Reinforced Concrete; 1984. p. 187–96.
[7] Kakemi M, Hannant DJ, Mulheron M. Filament fracture within glass fiber strands in hybrid fiber cement composites. J Mater Sci 1998;33:5375–82.
[8] Mobasher B, Li CY. Mechanical properties of hybrid cement based composites. ACI Mater J 1996;93(3):284–93.
[9] Perez-Pena M, Mobasher B. Mechanical properties of fiber reinforced lightweight concrete composites. Cem Concr Res J 1994;24(6):1121–32.
[10] Cyr MF, Peled A, Shah SP. Extruded hybrid fiber reinforced cementitious composites. In: Mansur MA, Ong KCG, editors. Proceedings FERRO-7. Singapore: ferrocement and thin fiber reinforced cement composites; 2001. p. 199–207.
[11] Peled A, Cyr M, Shah SP. Hybrid fibers in high performances extruded cement composites. In: Prisco MDi, Felicetti R, Plizzari GA, editors. Proceedings RILEM symposium. PRO 39: BEFIB; 2004. p. 139–48.
[12] Peled A, Mobasher B. Tensile behavior of fabric cement-based composites: pultruded and cast. ASCE J Mater Civ Eng 2007;19(4):340–8.
[13] Mobasher B, Peled A, Pahilajani J. Distributed cracking and stiffness degradation in fabric–cement composites. Mater Struct (RILEM) J 2006;39(3):317–31.
[14] Mobasher B, Pahilajani J, Peled A. Analytical simulation of tensile response of fabric reinforced cement based composites. J Cem Concr Compos 2006;28(1):77–89.
[15] Mobasher B. Micromechanical modeling of filament wound cement-based composites. ASCE J Eng Mech 2003;129(4):373–82.